



JAMA Neurol. 2020 Nov; 77(11): 1–10.

Published online 2020 Aug 3. doi: 10.1001/jamaneurol.2020.2231: 10.1001/jamaneurol.2020.2231

## Expanded Clinical Phenotype, Oncological Associations, and Immunopathologic Insights of Paraneoplastic Kelch-like Protein-11 Encephalitis

[Divyanshu Dubey](#), MD,<sup>1,2,3,4</sup> [Michael R. Wilson](#), MD, MAS,<sup>5</sup> [Benjamin Clarkson](#), PhD,<sup>2,4</sup> [Caterina Giannini](#), MD, PhD,<sup>1,4</sup> [Manish Gandhi](#), MD,<sup>1</sup> [John Cheville](#), MD,<sup>1</sup> [Vanda A. Lennon](#), MD, PhD,<sup>1,2,3,4</sup> [Scott Eggers](#), MD,<sup>2</sup> [Michelle F. Devine](#), MD,<sup>1,4</sup> [Caleigh Mandel-Brehm](#), PhD,<sup>6</sup> [Thomas Kryzer](#), AS,<sup>2,4</sup> [Shannon R. Hinson](#), PhD,<sup>2,4</sup> [Khashayarsha Khazaie](#), PhD,<sup>3</sup> [Chadwick Hales](#), MD, PhD,<sup>7</sup> [Jorge Kattah](#), MD,<sup>8</sup> [Kevin D. Pavelko](#), PhD,<sup>3</sup> [Patrick Andrews](#), BS,<sup>2,4</sup> [James E. Eaton](#), MD,<sup>9</sup> [Jiraporn Jitprapaikulsan](#), MD,<sup>4,10</sup> [John R. Mills](#), PhD,<sup>1,4</sup> [Eoin P. Flanagan](#), MD,<sup>1,2,4</sup> [Anastasia Zekeridou](#), MD, PhD,<sup>1,2,4</sup> [Bradley Leibovich](#), MD,<sup>11</sup> [James Fryer](#), MS,<sup>2,4</sup> [Matthew Torre](#), MD,<sup>12</sup> [Charles Kaufman](#), MD,<sup>13</sup> [James B. Thoreson](#), AS,<sup>1</sup> [Jessica Sagen](#), MA,<sup>1,2,4</sup> [Jenny J. Linnoila](#), MD, PhD,<sup>14</sup> [Joseph L. DeRisi](#), PhD,<sup>6,15</sup> [Charles L. Howe](#), PhD,<sup>2,3,4</sup> [Andrew McKeon](#), MD,<sup>1,2,4</sup> and [Sean J. Pittock](#), MD<sup>1,2,4</sup>

<sup>1</sup>Department of Laboratory Medicine and Pathology, Mayo Clinic, Rochester, Minnesota

<sup>2</sup>Department of Neurology, Mayo Clinic, Rochester, Minnesota

<sup>3</sup>Department of Immunology, Mayo Clinic, Rochester, Minnesota

<sup>4</sup>Center for MS and Autoimmune Neurology, Mayo Clinic, Rochester, Minnesota

<sup>5</sup>Weill Institute for Neurosciences, Department of Neurology, University of California, San Francisco

<sup>6</sup>Department of Biochemistry and Biophysics, University of California, San Francisco

<sup>7</sup>Department of Neurology, Emory University School of Medicine, Atlanta, Georgia

<sup>8</sup>Department of Neurology, University of Illinois College of Medicine, Peoria

<sup>9</sup>Department of Neurology, Vanderbilt University Medical Center, Nashville, Tennessee

<sup>10</sup>Department of Neurology, Mahidol University, Bangkok, Thailand

<sup>11</sup>Department of Urology, Mayo Clinic, Rochester, Minnesota

<sup>12</sup>Department of Pathology, Brigham and Women's Hospital, Boston, Massachusetts

<sup>13</sup>Louisiana Neurologic Consultants, Baton Rouge, Louisiana

<sup>14</sup>Department of Neurology, Massachusetts General Hospital, Boston

<sup>15</sup>Chan Zuckerberg Biohub, San Francisco, California

✉ Corresponding author.

[Article Information](#)

**Accepted for Publication:** April 1, 2020.

**Published Online:** August 3, 2020. doi:10.1001/jamaneurol.2020.2231

**Correction:** This article was corrected on September 14, 2020, to fix errors in Figures 2, 3, and 4.

**Corresponding Author:** Divyanshu Dubey, MD, Department of Neurology, Department of Laboratory Medicine and Pathology, Mayo Clinic, 200 First St SW, Rochester, MN 55905 ([dubey.divyanshu@mayo.edu](mailto:dubey.divyanshu@mayo.edu)).

**Conflict of Interest Disclosures:** Dr Dubey has received research support from Center of Multiple Sclerosis and Autoimmune Neurology, Center for Clinical and Translational Science, and Grifols pharmaceuticals. He has consulted for UCB and Astellas Pharmaceuticals. All compensation for consulting activities is paid directly to Mayo Clinic. Dr Dubey has a patent pending for Kelch-like protein 11 (KLHL11) IgG as a marker of neurological autoimmunity. Dr Wilson has received grants from Roche/Genentech, Sandler Foundation, William K. Bowes, Jr. Foundation, and from National Institutes of Health/National Institute of Neurological Disorders and Stroke (K08NS096117) during the conduct of the study; in addition, Dr Wilson had a patent to KLHL11 as neurological autoimmunity and paraneoplastic marker issued. Dr Clarkson reported grants from Mayo Clinic during the conduct of the study. Dr Lennon receives royalties from Mayo Clinic licensing of diagnostic tests for AQP4-IgG and is a named inventor on filed patents that relate to functional AQP4/NMO-IgG assays and NMO-IgG as a cancer marker. She has a patent pending for KLHL11, Septin 5 and MAP1B IgGs as markers of neurological autoimmunity and paraneoplastic disorders. Dr Mandel-Brehm has a patent pending for Kelch-like protein 11 IgG as a marker of neurologic autoimmunity. Dr Kryzer is a named inventor on filed patents that relate to functional AQP4/NMO-IgG assays and NMO-IgG as a cancer marker. He has a patent pending for KLHL11, Septin 5, and MAP1B IgGs as markers of neurological autoimmunity and paraneoplastic disorders. Dr Hales reported grants from the National Institutes of Health, BrightFocus Foundation, and the US Department of Defense during the conduct of the study. Dr Kattah reported other support from Otometrics during the conduct of the study. Dr Flanagan reported other support from Viela Bio outside the submitted work. Dr Zekeridou reported a patent to PDE10A-IgG as a biomarker of neurological autoimmunity pending. Dr Torre is currently supported by a T32 Training grant through the Pathology Department at Brigham and Woman's Hospital (T32 HL007627). Dr Linnoila is funded by National Institutes of Health/National Institute of Neurological Disorders and Stroke grant K08 NS101084, serves as an expert respondent for the National Vaccine Injury Compensation Program, and received honoraria from the American Academy of Neurology and the Massachusetts Neurologic Association for lectures on autoimmune neurology. Dr DeRisi has a patent pending for KLHL11 as a marker of neurologic autoimmunity. Dr McKeon has patent pending for KLHL11, Septin 5, and MAP1B as markers of neurological autoimmunity and paraneoplastic disorders. Dr Pittock is a named inventor on filed patents that relate to functional AQP4/NMO-IgG assays and NMO-IgG as a cancer marker. He has a patent pending for Septin 5 and MAP1B IgGs as markers of neurological autoimmunity and paraneoplastic disorders. He has consulted for Alexion and Medimmune. He has received research support from Grifols, Medimmune, and Alexion. All compensation for consulting activities is paid directly to Mayo Clinic. Dr Pittock has a patent pending for KLHL11-IgG as a marker of neurological autoimmunity. No other disclosures were reported.

**Additional Contributions:** We thank J. Schmeling, BS, and R. Johnson, MS, for technical support; S. Bryant, MS, and C. Smith for statistical support; and M. Curtis and S. Vinje for secretarial assistance. All are affiliated with the Mayo Clinic, and no compensation was received from a funding sponsor. We thank the Center for Multiple sclerosis and Autoimmune Neurology for storing and providing biospecimens for analysis. We thank the patients and their families for participation in this study.

Received 2019 Dec 16; Accepted 2020 Apr 1.

[Copyright](#) 2020 American Medical Association. All Rights Reserved.

## Key Points

---

### Question

What are the clinical, radiologic, immunopathologic, and human leukocyte antigen features of Kelch-like-protein-11 (KLHL11) encephalitis?

### Findings

In this case series, the common presenting feature of KLHL11 encephalitis is a rhombencephalitis phenotype with ataxia, diplopia, dysarthria, vertigo, hearing loss, and tinnitus. A strong oncologic association, KLHL11-specific T-cell response, human leukocyte antigen associations, and brain histopathology supports an immunopathologic basis.

## Meaning

Recognizing presenting features of KLHL11 encephalitis may aid in early diagnosis of this paraneoplastic syndrome and immunopathologic findings may guide immunotherapeutic management.

## Abstract

---

### Importance

Recognizing the presenting and immunopathological features of Kelch-like protein-11 immunoglobulin G seropositive (KLHL11 IgG+) patients may aid in early diagnosis and management.

### Objective

To describe expanding neurologic phenotype, cancer associations, outcomes, and immunopathologic features of KLHL11 encephalitis.

### Design, Setting, and Participants

This retrospective tertiary care center study, conducted from October 15, 1998, to November 1, 2019, prospectively identified 31 KLHL11 IgG+ cases in the neuroimmunology laboratory. Eight were identified by retrospective testing of patients with rhombencephalitis (confirmed by tissue-based-immunofluorescence and transfected-cell-based assays).

### Main Outcomes and Measures

Outcome variables included modified Rankin score and gait aid use.

### Results

All 39 KLHL11 IgG+ patients were men (median age, 46 years; range, 28-73 years). Initial clinical presentations were ataxia (n = 32; 82%), diplopia (n = 22; 56%), vertigo (n = 21; 54%), hearing loss (n = 15; 39%), tinnitus (n = 14; 36%), dysarthria (n = 11; 28%), and seizures (n = 9; 23%). Atypical neurologic presentations included neuropsychiatric dysfunction, myeloneuropathy, and cervical amyotrophy. Hearing loss or tinnitus preceded other neurologic deficits by 1 to 8 months in 10 patients (26%). Among patients screened for malignancy (n = 36), testicular germ-cell tumors (n = 23; 64%) or testicular microlithiasis and fibrosis concerning for regressed germ cell tumor (n = 7; 19%) were found in 83% of the patients (n = 30). In 2 patients, lymph node biopsy diagnosed metastatic lung adenocarcinoma in one and chronic lymphocytic leukemia in the other. Initial brain magnetic resonance imaging revealed T2 hyperintensities in the temporal lobe (n = 12), cerebellum (n = 9), brainstem (n = 3), or diencephalon (n = 3). Among KLHL11 IgG+ patients who underwent HLA class I and class II genotyping (n = 10), most were found to have *HLA-DQB1\*02:01* (n = 7; 70%) and *HLA-DRB1\*03:01* (n = 6; 60%) associations. A biopsied gadolinium-enhancing temporal lobe lesion demonstrated T cell–predominant inflammation and nonnecrotizing granulomas. Cerebellar biopsy (patient with chronic ataxia) and 2 autopsied brains demonstrated Purkinje neuronal loss and Bergmann gliosis, supporting early active inflammation and later extensive neuronal loss. Compared with nonautoimmune control peripheral blood mononuclear cells, cluster of differentiation (CD) 8+ and CD4+ T cells were significantly activated when patient peripheral blood mononuclear cells were cultured with KLHL11 protein. Most patients (58%) benefitted from

immunotherapy and/or cancer treatment (neurological disability stabilized [n = 10] or improved [n = 9]). Kaplan-Meier curve demonstrated significantly higher probability of wheelchair dependence among patients without detectable testicular cancer. Long-term outcomes in KLHL11-IgG+ patients were similar to Ma2 encephalitis.

## Conclusions and Relevance

Kelch-like protein-11 IgG is a biomarker of testicular germ-cell tumor and paraneoplastic neurologic syndrome, often refractory to treatment. Described expanded neurologic phenotype and paraclinical findings may aid in its early diagnosis and treatment.

## Introduction

---

Numerous neural autoantibody biomarkers of paraneoplastic encephalitis have been defined in the past decade, and new autoantibodies continue to be discovered.<sup>1,2</sup> Many serve as biomarkers for specific cancer types.<sup>3</sup> In 2019,<sup>4</sup> we described the index case of a new paraneoplastic autoimmune Kelch-like protein-11 (KLHL11) encephalitis associated with seminoma and summarized clinical findings for 12 additional cases.

The 26 additional patients we report here provide a more comprehensive overview of the clinical phenotype, its initial presentation, neurologic findings, oncologic associations, and disability outcomes. We also investigated human leukocyte antigen (HLA) haplotype associations and KLHL11-specific T-cell responses and performed immunopathologic analyses of autopsied and biopsied central nervous system (CNS) tissues.

## Methods

---

### Identification of Patients

This is a retrospective, clinical-serological cohort study approved by the institutional review board of Mayo Clinic, with a waiver of consent for clinical data obtained as part of serologic test validation (study 08-00647). All Mayo Clinic patients whose medical records were analyzed provided written consent for medical research.

The Mayo Clinic Neuroimmunology Laboratory tested serum and cerebrospinal fluid (CSF) specimens submitted from patients being evaluated on a service basis for a suspected paraneoplastic neurological or autoimmune encephalitic illness. Between January 1, 1998, and November 1, 2019, the mouse tissue-based immunofluorescence assay (IFA) component of the laboratory's standard serologic testing algorithm prospectively identified 31 cases exhibiting the "Sparkles" IFA pattern<sup>4</sup> characteristic of KLHL11-IgG reactivity. Eight additional cases with characteristic Sparkles IFA pattern were identified retrospectively by testing stored serum or CSF samples from 89 Mayo Clinic patients presenting with ataxia or rhombencephalitis who were previously formally reported seronegative. Here we confirmed that all 39 sera were KLHL11-immunoglobulin G-positive using a HEK293 KLHL11 overexpression cell-based assay (CBA) (eAppendix in the [Supplement](#)) and additionally tested them for Ma2-IgG by enzyme-linked immunosorbent assay.

### Comparative Group

As a control group, we used archival specimens from 22 Ma2-IgG-seropositive patients identified in the Mayo Neuroimmunology laboratory database; 3 were included in previous studies.<sup>5,6,7</sup> The Ma2-IgG-positive cases were all negative for KLHL11-IgG by IFA. Full details of methods pertaining to IFAs on rodent brain tissue, HEK 293T-cell overexpression assays, Ma2 enzyme-linked immunosorbent assay, dendritic cell/T-cell assay, mass cytometry, HLA

typing, and statistical analysis are provided in the eMethods in the [Supplement](#). Fisher exact test and Mann-Whitney *U* test were used to analyze nominal and continuous variables, respectively (SPSS, version 25; IBM). The *P* value was 2-sided, and values of less than .05 were considered significant.

## Results

---

Kelch-like protein-11 IgG was detected in serum and/or CSF of 39 patients, initially by tissue-based IFA (eFigure 1A and B in the [Supplement](#)), and specificity was subsequently confirmed by transfected cell-based assay (eFigure 2A and B in the [Supplement](#)). All patients (including 13 previously reported<sup>4</sup>) were male, and their median age was 46 years (range, 28-73 years). Median serum and CSF titers by IFA were 1:30 720 (1:960 to 1:245 760) and greater than 1:640, respectively. All KLHL11-IgG-positive specimens were negative for Ma2-IgG.

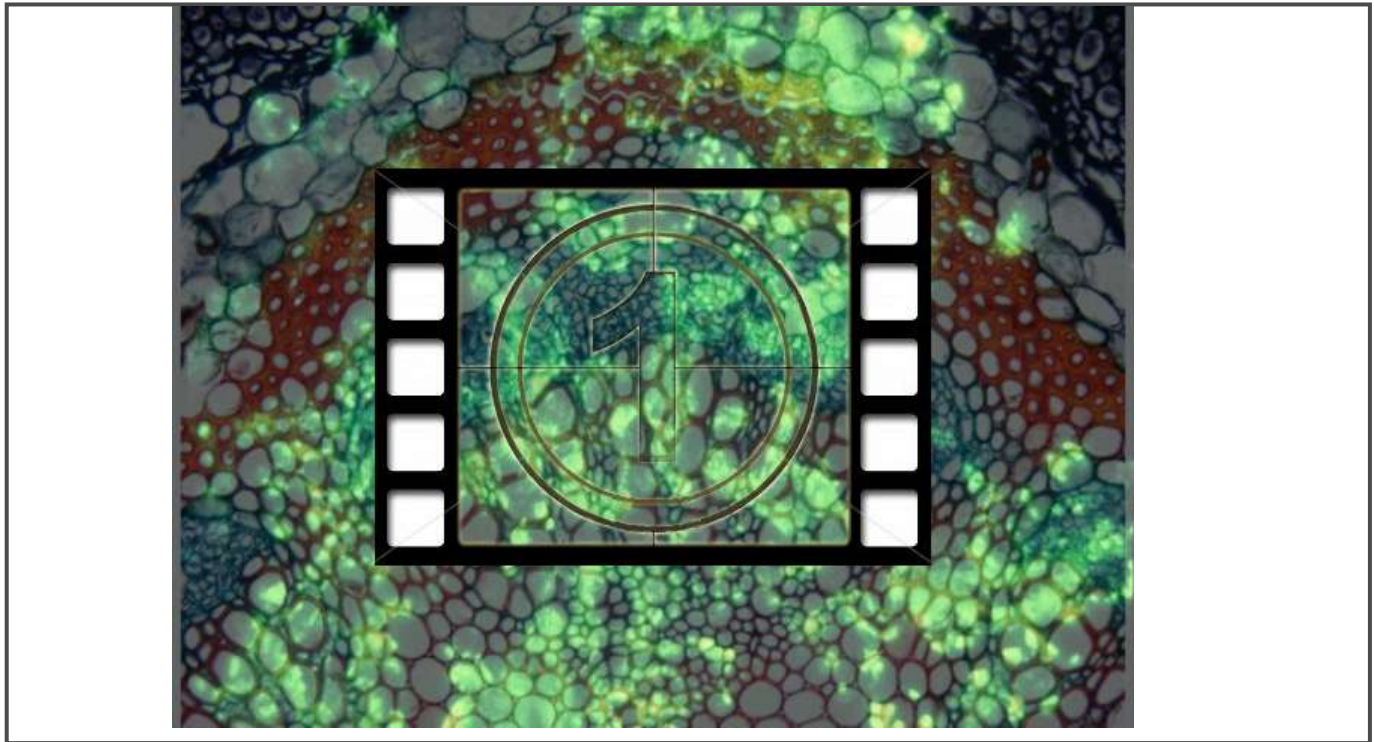
## Clinical Presentation

In 28 of 39 cases, the predominant clinical presentation was paraneoplastic rhomboencephalitis (brainstem encephalitis and/or cerebellitis); 5 presented with a combination of paraneoplastic rhombencephalitis and limbic encephalitis; and 6 presented with only limbic encephalitis. Most patients presented with gait instability (n = 32; 82%) and diplopia (n = 22; 56%). It is noteworthy that vertigo (n = 21; 54%), hearing loss (n = 15; 39%), and tinnitus (n = 14; 36%) were a common and distinctive clinical symptom among patients with autoimmune KLHL11 encephalitis. In 26% of cases, hearing loss or tinnitus preceded other neurologic deficits (by a median of 2.5 months; range, 1-8 months). Seizures and encephalopathy were a component of the presenting manifestations in 9 patients (23%), 4 of whom had coexisting brainstem or cerebellar dysfunction.

On examination, the most common neurologic deficits were gait ataxia (n = 32; 82%; [Video 1](#)), dysmetria (n = 24; 62%), nystagmus (n = 21; 54%; [Video 2](#)), nuclear or supranuclear gaze palsy (n = 13; 33%), dysarthria (n = 11; 28%, [Video 3](#)), and tremors (n = 12; 31%). Almost one-third of patients had brisk deep tendon reflexes (n = 13; 33%).

Video 1.

Gait Ataxia in Autoimmune Kelch-like Protein 11 Encephalitis

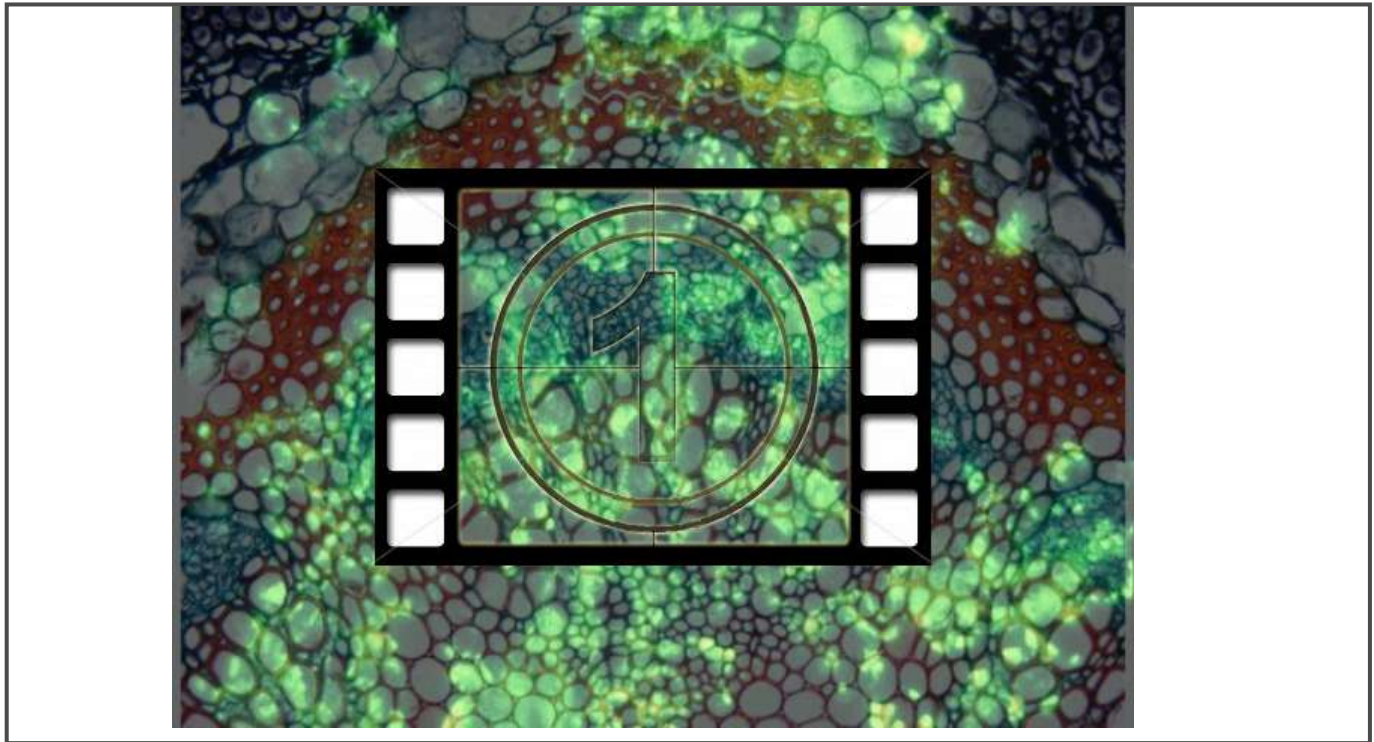


[Download](#) video file. (44M, mp4)



Video 2.

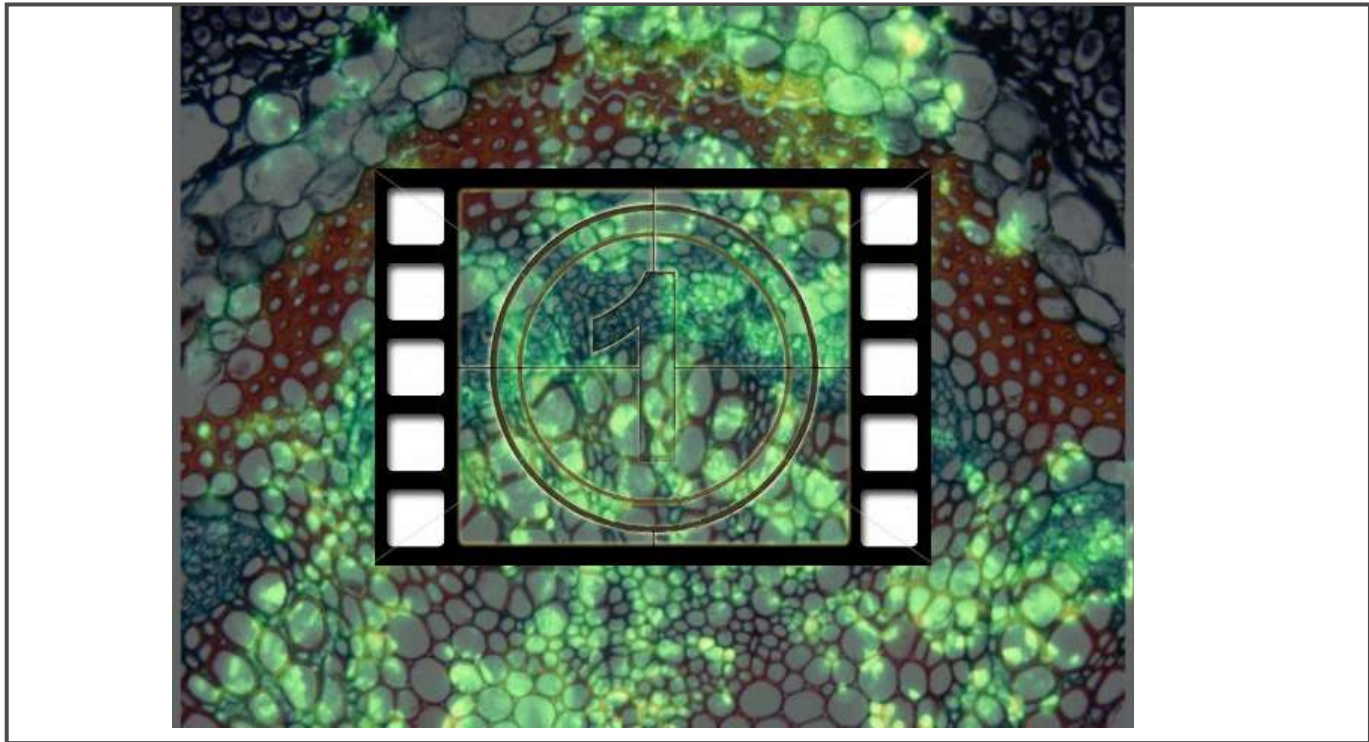
Nystagmus in Autoimmune Kelch-like Protein 11 Encephalitis



[Download](#) video file. (73M, mp4)

### Video 3.

#### Dysarthria in Autoimmune Kelch-like Protein 11 Encephalitis



[Download](#) video file. (31M, mp4)

#### Rare Presentations Encountered in 4 Patients

Neuropsychiatric presentations were prominent in 2 patients and included anxiety and panic attacks. As the disease progressed, ataxia, sensorineural hearing loss, and right-sided trigeminal neuropathy developed in 1 of those patients; severe refractory facial pain and paraesthesias evolved over a period of 2 years. In the second patient with early neuropsychiatric manifestations, the evolution of diffuse fasciculations, progressive cognitive decline, and ataxia over the next 3 years led to initial misdiagnoses of frontotemporal dementia and amyotrophic lateral sclerosis. In the next 2 years, supranuclear gaze palsy, ataxia, dysarthria, and dysphagia developed. A third patient presented with subacute flaccid paraparesis and magnetic resonance imaging (MRI) demonstrated an ill-defined T2/fluid-attenuated inversion recovery (FLAIR) hyperintensity in the thoracic cord, and enhancement of lumbar roots. Electrodiagnostic testing confirmed that he had polyradiculoneuropathy. Nystagmus, supranuclear gaze palsy, dysarthria, and ataxia developed within 2 years of initial presentation. A fourth patient had asymmetric cervical amyotrophy with profound upper limb weakness in addition to features of rhombencephalitis (nystagmus, vertigo, and ataxia). A testicular seminoma was detected in all 4 cases.

#### Cerebrospinal Fluid Analysis

Results of CSF analysis were available for 34 cases. Findings were inflammatory in 85% (n = 29): protein 50 mg/dL or greater (to convert to grams per liter, multiply by 10); leukocyte counts exceeding 5 cells/ $\mu$ L (to convert to  $\times 10^9$  per liter, multiply by 10); or both. The median leukocyte count was 10 cells/ $\mu$ L (range: 0-86 cells/ $\mu$ L), and median total protein was 65 mg/dL (23-200 mg/dL). Supernumerary oligoclonal bands were detected in 18 of 22 evaluated patients' specimens (82%; median, 6; range, 0-14).



## Neuroimaging

Among 37 patients with an available brain MRI at time of diagnosis, 7 had no detected abnormality ([Figure 1](#)). Twenty-eight patients (76%) had T2/FLAIR hyperintensity (temporal lobe, n = 12; cerebellum, n = 9; brainstem, n = 3; and diencephalon, n = 3; [Figure 2](#)). One patient had midbrain T2 hyperintensity on brain MRI along with bilaterally symmetric T2 signal abnormality involving central gray structures extending to the upper thoracic spinal cord. Three patients had gadolinium enhancement on MRI (temporal lobe, n = 2; and midbrain and lumbosacral roots, n = 1; [Figure 2](#)). In 2 patients lacking evidence of brain parenchymal T2 hyperintensity, gadolinium enhancement was noted in leptomeninges (n = 1) and trigeminal nerve (n = 1). Of 12 patients with follow-up imaging more than 2 years after the initial MRI brain, 6 had cerebellar atrophy, 2 had medial temporal lobe atrophy, and 1 had diffuse cerebral atrophy. Three patients had hypertrophic olivary degeneration.

## Audiology

Sensorineural hearing loss was demonstrated in all 7 tested patients (eFigure 3 in the [Supplement](#)).

## Alternative Diagnosis

Before a paraneoplastic etiology was considered, 21 patients (54%) were assigned varied alternative diagnosis, including infectious encephalitis (n = 6; Whipple disease in 4), brain tumor (n = 3), alcoholic cerebellar degeneration (n = 2), multiple sclerosis (n = 2), medication toxicity (n = 1), Wernicke encephalopathy (n = 1), neurosarcoidosis (n = 1), ischemic stroke (n = 1), Alzheimer disease (n = 1), frontotemporal degeneration/amyotrophic lateral sclerosis (n = 1), benign paroxysmal positional vertigo (n = 1), and functional neurological disorder (n = 1). Testicular cancer was diagnosed in most patients who had follow-up information (n = 13 of 20; 65%) after their physicians were informed about the high frequency of testicular cancer association in patients whose serum was scored positive for the Sparkles immunostaining pattern.

## Human Leukocyte Antigen Association

Among KLHL11-IgG seropositive patients who underwent HLA class I and class II genotyping (n = 10), most had *DQB1\*02:01* (n = 7; 70%) and *DRB1\*03:01* (n = 6; 60%) associations. A common major histocompatibility complex class II HLA haplotype, *DRB1\*03:01-DQB1\*02:01* (*DR17* [3] to *DQ2*), was found in 6 of 10 evaluated patients with autoimmune KLHL11 encephalitis. Other haplotypes detected were *DQ6-DR13* (n = 3; *DRB1\*1302-DQB1\*06:04* [n = 1] and *DRB1\*1301-DQB1\*06:03* [n = 2]) and *DR7-DQ2* (n = 1; *DRB1\*0701-DQB1\*02:01*). These latter 4 patients did not obviously differ in clinical presentation, cancer association, or clinical outcome from the *DRB1\*03:01-DQB1\*02:01* haplotype-positive patients. Among 6 patients with a common haplotype, 3 had seminoma (2 testicular and 1 extratesticular [mediastinal]), 1 had a lung adenocarcinoma, and 2 had testicular microlithiasis and fibrosis. The 4 patients with alternate haplotypes had seminoma.

## KLHL11-Specific T Cells

Peripheral blood mononuclear cell (PBMC)-derived dendritic cell/T cell cocultures were treated with full length KLHL11 or vehicle only for 72 hours ([Figure 2A](#)), and surface expression of the activation marker cluster of differentiation 69 (CD69) was measured on CD4+ and CD8+ T cell subsets by flow cytometry. Compared with vehicle, the change in percentage of CD4+ and CD8+ T cells expressing CD69 was determined for 5 KLHL11+ patients and 12 healthy control individuals. As shown in [Figure 2B](#), we observed a marked increase in CD69-expressing T cells among both CD4+ and CD8+ T-cell subsets in patients compared with healthy control individuals. The KLHL11

seropositive patients' PBMC-derived T cell cocultures did not exhibit increased frequency of CD69-expressing CD8+ or CD4+ T cells in response to treatment with full-length paraneoplastic antigen Ma2 protein (eFigure 4 in the [Supplement](#)). In 1 patient, we also performed cytometry by time of flight using a 31-analyte T-cell panel to more fully characterize the profile of T-cell subsets following KLHL11 treatment. As shown ([Figure 2C](#)), we observed marked expansion of T-effector memory subsets as well as CD25+CD28+CD8+effector and CD25+CD28+CD4+effector subsets.

## Neuropathology

Brain tissue was available from 4 patients (2 biopsies and 2 autopsies). A gadolinium-enhancing right temporal lobe lesion from a patient presenting with headache and cognitive decline exhibited chronic lymphocytic (T-cell predominant) inflammation with nonnecrotizing granulomas ([Figure 3A-F](#)). A cerebellar biopsy from another patient presenting with chronic ataxia and nystagmus whose brain MRI showed cerebellar atrophy demonstrated Bergmann gliosis and Purkinje neuronal loss, with a small collection of inflammatory cells (case not shown). Findings in this patient were consistent with the histopathology found in the 2 autopsied brains (1 patient presenting with gait ataxia and the other presenting with neuropsychiatric manifestations and diplopia). The cerebellum in both cases demonstrated moderate to severe loss of Purkinje neurons accompanied by Bergmann gliosis (eFigure 5 in the [Supplement](#)). One patient had gliotic changes in the left thalamus (eFigure 5 in the [Supplement](#)) localized to the region of thalamic FLAIR/T2 hyperintensity. The other patient had severe degeneration of the inferior olivary and cerebellar dentate nuclei and severe neuronal loss and gliosis in the hippocampal CA1 layer. The neuropathologic findings suggest a disease continuum with early-stage active inflammation and severe neuronal loss in the chronic stage.

## Oncologic Associations

A neoplasm was detected in 25 of 36 patients who were screened for cancer (computed tomography chest/abdomen/pelvis and testicular ultrasonography). Testicular cancer was found in 23 cases (seminoma in 21). Four of the seminomas were found in an extratesticular locations by whole-body positron emission tomography (2 mediastinal and 2 retroperitoneal). The neoplasm in the 2 other testicular cancer patients were mixed germ cell tumors (1 seminoma and embryonal carcinoma; 1 embryonal carcinoma). One patient had lung adenocarcinoma and another had chronic lymphocytic leukemia. Scrotal ultrasonography revealed testicular microlithiasis in 7 patients. Orchiectomy in those patients demonstrated a fibrotic mass with scattered lymphocytes and calcification consistent with an immunologically eliminated (regressed or burned-out) testicular germ cell tumor.<sup>8,9,10,11</sup>

The seminoma tissue immunohistopathology from a patient with autoimmune KLHL11 encephalitis demonstrated T-cell predominant lymphocytic infiltration ([Figure 3G and H](#)). Furthermore, KLHL11 immunoreactivity was detected in the tumor cell cytoplasm ([Figure 3I](#)). We also demonstrated KLHL11 immunoreactivity in the lymph node biopsy of the patient with metastatic lung adenocarcinoma (eFigure 6A and B in the [Supplement](#)).

## Clinical Outcomes

Nearly all patients with clinical follow-up duration of at least 6 months (n = 32 of 33; median period, 30 months [range, 6-216 months]) received 1 or more of the following as initial immunotherapy: intravenous methylprednisolone (IVMP; n = 27), intravenous immune globulin (IVIg; n = 15), plasmapheresis (n = 10), or oral prednisone for more than 2 weeks (n = 6). A subset of 17 patients received second-line immunosuppressive therapy with 1 or more of the following agents: cyclophosphamide (n = 13), rituximab (n = 5), mycophenolate mofetil (n = 2), azathioprine (n = 1), tacrolimus (n = 1), or natalizumab (1). Twenty-four patients received surgery, chemotherapy, or radiation therapy for management of a diagnosed cancer. Nineteen patients (58%) stabilized neurologically (n = 10) or improved (n = 9). At last follow-up, 21 patients (57%) needed a gait aid (wheelchair, n = 16; roller walker, n = 5).

The median mRS at last assessment was 4 (range, 2-6). Significantly fewer patients with testicular cancer required a wheelchair at last follow-up (44% [n = 7] vs 90% [n = 9] without cancer detection; OR, 0.09; 95% CI, 0.01-0.85;  $P = .02$ ), suggesting less neurologic morbidity among cases with confirmed (and treated) testicular cancer. Consistent with this conclusion was the observation that there was a trend toward neurologic deficits stabilizing or improving more frequently in patients treated for testicular cancer than in patients without a detectable testicular cancer. However, the trend was not statistically significant (68% [n = 16] vs 36% [n = 4];  $P = .08$ ). Kaplan-Meier curve analysis demonstrated significantly higher probability of wheelchair dependence among patients without detectable testicular cancer ([Figure 4A](#)). Eight deaths were reported, with a median interval of 55 months from symptom onset to death (range, 10-109 months).

### Comparison With Ma2-IgG Seropositive Cases

The frequency of autoimmune rhombencephalitis diagnosis among KLHL11-IgG seropositive patients was significantly higher than among a comparison cohort of patients seropositive for Ma2-IgG, another neural autoantibody recognized as a marker of paraneoplastic rhombencephalitis associated with testicular cancer (82% [n = 32] vs 40% [n = 8]; OR, 3.2; 95% CI, 1.6-6.4;  $P = .003$ ; [Table](#)). Furthermore, symptoms of ataxia (82% [n = 32] vs 30% [n = 6];  $P < .001$ ), vertigo (54% [n = 21] vs 15% [n = 3];  $P = .005$ ), hearing loss (39% [n = 15] vs 0;  $P = .001$ ), and tinnitus (36% [n = 14] vs 0;  $P = .001$ ) were significantly more common among patients with autoimmune KLHL11 encephalitis, and histopathologic diagnosis of seminoma was significantly more frequent among KLHL11-IgG encephalitis cases (58% [n = 21] vs 11% [n = 2]; OR, 5.9; 95% CI 1.5-23.3;  $P = .001$ ). Kaplan-Meier curve demonstrated similar probability of wheelchair dependence among KLHL11-IgG and Ma2-IgG seropositive patients ([Figure 4B](#)).

## Discussion

---

The autoantibody that we have defined as a new serologic biomarker of paraneoplastic encephalitis in men is KLHL11-specific IgG that is highly associated with testicular germ cell tumors. The typical clinical presentation is rhombencephalitis, with predominant ataxia, diplopia, dysarthria, hearing loss, tinnitus, and vertigo. Hearing loss and tinnitus appear to be relatively unique manifestations of paraneoplastic KLHL11 encephalitis. In some cases, these symptoms preceded other neurologic symptoms and signs by weeks or months. A subset of patients had limbic encephalitis at presentation. Although initially normal in a considerable minority of patients, brain MRI often demonstrated T2/FLAIR abnormalities involving the brainstem or limbic system. Some brain MRIs resembled prominent mass lesions, leading to an initial misdiagnosis of CNS malignancy or metastasis. The prominence of supernumerary oligoclonal bands in CSF of most patients with autoimmune KLHL11 encephalitis (evidence of intrathecal IgG synthesis) is consistent with paraneoplastic neurologic autoimmunity being the outcome of reactivation of T and B lymphocytes by neural cell antigens on entering the CNS, which were initially activated by tumor antigens in the periphery.

Histopathologic evaluation of 1 patient with a gadolinium-enhancing temporal lobe lesion showed large inflammatory collections and nonnecrotizing granulomas. On the other hand, neuropathologic evaluation of 3 patients with chronic rhombencephalitis (2 autopsies and 1 brain biopsy) demonstrated Purkinje cell loss and Bergmann gliosis, with limited inflammation. This suggests a disease continuum with active inflammation early and severe neuronal loss in the chronic stage. A T cell–predominant infiltrate found within the seminoma ([Figure 3G](#) and [H](#)) of 1 patient supports the hypothesis that neurologic autoimmunity is initiated as an autoreactive T-cell response by an onconeural antigen expressed in a patient's tumor. In line with this, we observed an increased frequency of KLHL11 antigen-specific T cell among patient PBMCs compared with those from healthy control individuals, and these T cells exhibited predominantly effector or effector memory phenotypes on antigen stimulation. It will be important to ascertain whether these peripheral T cells are clonally associated with brain-infiltrating T cells or CSF T cells in patients with

KLHL11 encephalitis. CD8 T-cell infiltration on brain histopathology ([Figure 3F](#)) and autoantigen-specific CD8+ T cell activations, suggest that cytotoxic T-cell mediated disease pathogenesis of KLHL11 encephalitis seems to resemble other classic paraneoplastic neurologic syndromes.<sup>12</sup>

Despite their common oncologic association with testicular germ cell tumors, paraneoplastic autoimmune Ma2<sup>13</sup> and KLHL11 encephalitis appear to be immunologically distinct syndromes. Symptoms of ataxia, vertigo, hearing loss, and tinnitus are more common with KLHL11 encephalitis than with Ma2 encephalitis, and KLHL11 encephalitis associates more strongly with seminoma than does Ma2 encephalitis. However, as reported for Ma2 encephalitis,<sup>13</sup> patients with KLHL11 encephalitis in whom a testicular germ cell tumor is found appear to have a more favorable prognosis.

Only 25% of cases were noted to improve neurologically following cancer treatment and/or immunotherapy. Ataxia, eye movement abnormalities, and hearing loss were all refractory to treatment. The refractory nature of KLHL11 rhombencephalitis is similar to other classic paraneoplastic syndromes such as antineuronal nuclear antibody type 1 (aka anti-Hu) IgG associated limbic encephalitis,<sup>14</sup> Purkinje cell antibody type 1 (aka anti-Yo) IgG-associated paraneoplastic cerebellar degeneration,<sup>15,16</sup> and Ma2 encephalitis.<sup>13</sup> Kelch-like protein-11 IgG is unlikely to be directly pathogenic given the intracellular localization of the KLHL11 autoantigen. The presumed presentation of testicular tumor-derived KLHL11 peptides ([Figure 3C](#)) by activated antigen-presenting dendritic cells is thought to initially prime antigen-specific CD4+ helper T cells, and this hypothesis is supported by the strong HLA class II association we documented in this study. CD4 T cell activation in turn activates CD8+ effector cells and autoantibody-producing B cells.<sup>17</sup> The resulting potent cytotoxic T cell response would have potential to attack both tumor cells and neurons expressing surface upregulated KLHL11 peptides. The T-cell predominant infiltrates observed in both brain and tumor tissues obtained from these patients support this mechanism of disease pathogenesis ([Figure 3](#)). Because testicular cancer is incriminated as the source of autoantigen-driving autoimmune KLHL11 encephalitis, cancer surveillance and appropriate management are indicated. The fact that patients in whom testicular cancer was diagnosed and treated had a more favorable clinical outcome supports this hypothesis. Furthermore, inhibition of antigen presentation by blockade of KLHL11-specific HLA alleles or haplotype on antigen-presenting cells with peptide ligands may also be explored as a therapeutic strategy for this refractory neurologic disorder.<sup>18,19</sup>

## Limitations

It is impossible to estimate how many cases of this type of autoimmune encephalitis may have been missed by tissue-based serologic screening, given the sparse immunofluorescence staining pattern.<sup>4</sup> Therefore, we analyzed the clinical specificity of a high throughput method of cell-based assay screening with subsequent tissue-based IFA confirmation (eTable and eFigure 2 in the [Supplement](#)). Prior studies have highlighted the importance of combining both CBA and brain immunohistochemistry for defining *N*-methyl-D-aspartate receptor IgG,<sup>20</sup> Glial fibrillary acidic protein-IgG<sup>21</sup> and neurofilament-light chain-IgG positivity.<sup>22</sup> The use of CBA methods alone to identify and confirm autoantibody biomarkers targeting linear intracellular epitopes is not common practice in clinical service laboratories and may result in false-positive results. In this study, we detected 3 control cases (eTable in the [Supplement](#)) that tested positive on KLHL11 CBA but negative on tissue IFA and phage immunoprecipitation sequencing (eTable in the [Supplement](#)). All patients with KLHL11 encephalitis we report here had a positive and highly stereotyped Sparkles tissue-based IFA pattern (eFigure 1 in the [Supplement](#)). This IFA pattern colocalizes with a commercial antibody to KLHL11.<sup>4</sup> It is important to note that in a 2020 study analyzing KLHL11 antibodies,<sup>23</sup> only 22% of the patients had positive rat brain immunohistochemistry. Also, the IFA pattern represented in this article did not resemble the Sparkles pattern described here (eFigure 1 in the [Supplement](#)), making it unclear whether these patients' antibodies were targeting the highly conserved epitope targeted by the autoantibodies in patients with KLHL11. It is not uncommon for a broader neurologic phenotype to emerge once testing for a novel paraneoplastic antibody is incorporated into standard paraneoplastic serologic testing,<sup>24,25</sup> but we suggest confirmation of all cases by tissue-based assays to optimize clinical specificity.

Retrospective study design, varying treatment strategies, and follow-up durations are other limitations of our study. Common HLA allele and haplotype associations are based on a limited number of cases, and larger future studies are required to confirm these associations.

## Conclusions

---

Kelch-like protein-11 IgG is a new paraneoplastic autoantibody biomarker associated with testicular germ cell tumor and an incapacitating rhomboencephalitis that is often refractory to treatment. Our study describes the various clinical presentations and immunopathologic findings that may aid in its early diagnosis and appropriate treatment.

## Notes

---

Supplement.

**eMethods.**

**eAppendix.** Assay performance characteristics

**Table.** Healthy and disease controls tested on KLHL11 cell based assay

**eFigure 1.** KLHL 11 patient IgG rodent brain tissue indirect immunofluorescence assay

**eFigure 2.** KLHL11 patient IgG binds specifically to GFP-tagged KLHL11 foci in transfected

**eFigure 3.** Quantification of eye movement abnormalities and sensorineural hearing loss in a patient with autoimmune KLHL11 encephalitis

**eFigure 4.** Autoantigen specific T-cell activation

**eFigure 5.** Autopsy of two patients (Case A-B, Case C-F) with chronic cerebellar ataxia and thalamic lesions

**eFigure 6.** Immunohistochemical staining of lung adenocarcinoma from KLHL11 encephalitis patient

## References

---

1. Dalmau J, Geis C, Graus F. Autoantibodies to synaptic receptors and neuronal cell surface proteins in autoimmune diseases of the central nervous system. *Physiol Rev.* 2017;97(2):839-887. doi:10.1152/physrev.00010.2016 [PMCID: PMC5539405] [PubMed: 28298428] [CrossRef: 10.1152/physrev.00010.2016]
2. Dubey D, Pittock SJ, Kelly CR, et al. . Autoimmune encephalitis epidemiology and a comparison to infectious encephalitis. *Ann Neurol.* 2018;83(1):166-177. doi:10.1002/ana.25131 [PMCID: PMC6011827] [PubMed: 29293273] [CrossRef: 10.1002/ana.25131]
3. Pittock SJ, Kryzer TJ, Lennon VA. Paraneoplastic antibodies coexist and predict cancer, not neurological syndrome. *Ann Neurol.* 2004;56(5):715-719. doi:10.1002/ana.20269 [PubMed: 15468074] [CrossRef: 10.1002/ana.20269]
4. Mandel-Brehm C, Dubey D, Kryzer TJ, et al. . Kelch-like protein 11 antibodies in seminoma-associated paraneoplastic encephalitis. *N Engl J Med.* 2019;381(1):47-54. doi:10.1056/NEJMoa1816721 [PMCID: PMC6800027] [PubMed: 31269365] [CrossRef: 10.1056/NEJMoa1816721]

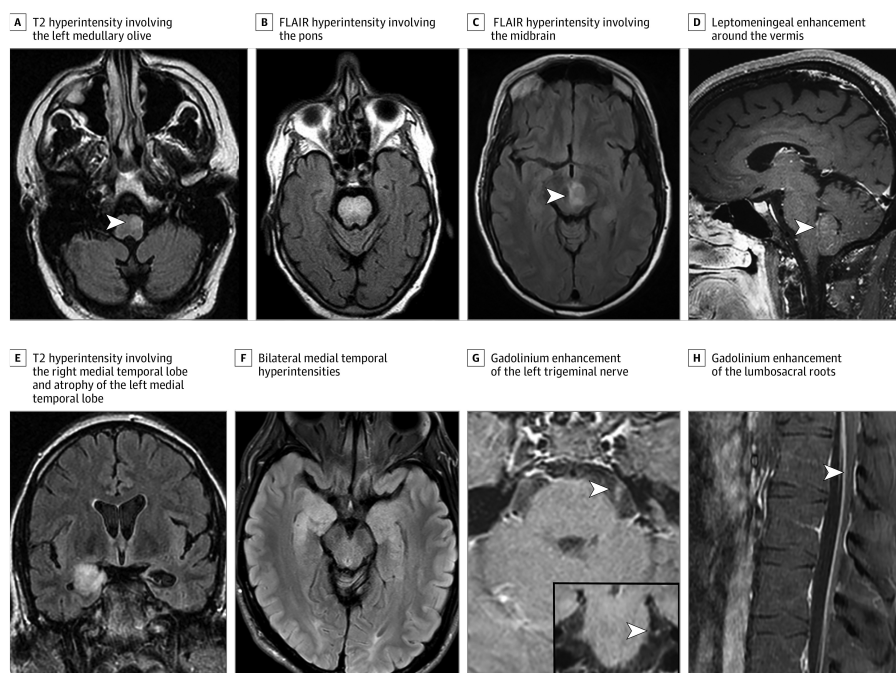


5. Adams C, McKeon A, Silber MH, Kumar R. Narcolepsy, REM sleep behavior disorder, and supranuclear gaze palsy associated with Ma1 and Ma2 antibodies and tonsillar carcinoma. *Arch Neurol*. 2011;68(4):521-524. doi:10.1001/archneurol.2011.56 [PubMed: 21482933] [CrossRef: 10.1001/archneurol.2011.56]
6. Quek AM, Britton JW, McKeon A, et al. . Autoimmune epilepsy: clinical characteristics and response to immunotherapy. *Arch Neurol*. 2012;69(5):582-593. doi:10.1001/archneurol.2011.2985 [PMCID: PMC3601373] [PubMed: 22451162] [CrossRef: 10.1001/archneurol.2011.2985]
7. English SW, Keegan BM, Flanagan EP, Tobin WO, Zalewski NL. Clinical reasoning: a 30-year-old man with headache and sleep disturbance. *Neurology*. 2018;90(17):e1535-e1540. doi:10.1212/WNL.0000000000005356 [PubMed: 29686126] [CrossRef: 10.1212/WNL.0000000000005356]
8. Balzer BL, Ulbright TM. Spontaneous regression of testicular germ cell tumors: an analysis of 42 cases. *Am J Surg Pathol*. 2006;30(7):858-865. doi:10.1097/01.pas.0000209831.24230.56 [PubMed: 16819328] [CrossRef: 10.1097/01.pas.0000209831.24230.56]
9. Balalaa N, Selman M, Hassen W. Burned-out testicular tumor: a case report. *Case Rep Oncol*. 2011;4(1):12-15. doi:10.1159/000324041 [PMCID: PMC3114614] [PubMed: 21691568] [CrossRef: 10.1159/000324041]
10. Ishikawa H, Kawada N, Taniguchi A, et al. . Paraneoplastic neurological syndrome due to burned-out testicular tumor showing hot cross-bun sign. *Acta Neurol Scand*. 2016;133(5):398-402. doi:10.1111/ane.12469 [PubMed: 26248690] [CrossRef: 10.1111/ane.12469]
11. Freifeld Y, Kapur P, Chitkara R, Lee F, Khemani P, Bagrodia A. Metastatic “burned out” seminoma causing neurological paraneoplastic syndrome-not quite “burned out”. *Front Neurol*. 2018;9:20. doi:10.3389/fneur.2018.00020 [PMCID: PMC5797537] [PubMed: 29441039] [CrossRef: 10.3389/fneur.2018.00020]
12. Darnell RB, Posner JB. Paraneoplastic syndromes affecting the nervous system. *Semin Oncol*. 2006;33(3):270-298. doi:10.1053/j.seminoncol.2006.03.008 [PubMed: 16769417] [CrossRef: 10.1053/j.seminoncol.2006.03.008]
13. Dalmau J, Graus F, Villarejo A, et al. . Clinical analysis of anti-Ma2-associated encephalitis. *Brain*. 2004;127(Pt 8):1831-1844. doi:10.1093/brain/awh203 [PubMed: 15215214] [CrossRef: 10.1093/brain/awh203]
14. Dalmau J, Graus F, Rosenblum MK, Posner JB. Anti-Hu--associated paraneoplastic encephalomyelitis/sensory neuropathy. a clinical study of 71 patients. *Medicine (Baltimore)*. 1992;71(2):59-72. doi:10.1097/00005792-199203000-00001 [PubMed: 1312211] [CrossRef: 10.1097/00005792-199203000-00001]
15. Rojas I, Graus F, Keime-Guibert F, et al. . Long-term clinical outcome of paraneoplastic cerebellar degeneration and anti-Yo antibodies. *Neurology*. 2000;55(5):713-715. doi:10.1212/WNL.55.5.713 [PubMed: 10980743] [CrossRef: 10.1212/WNL.55.5.713]
16. Jones AL, Flanagan EP, Pittock SJ, et al. . Responses to and outcomes of treatment of autoimmune cerebellar ataxia in adults. *JAMA Neurol*. 2015;72(11):1304-1312. doi:10.1001/jamaneurol.2015.2378 [PubMed: 26414229] [CrossRef: 10.1001/jamaneurol.2015.2378]
17. Darnell RB. Onconeural antigens and the paraneoplastic neurologic disorders: at the intersection of cancer, immunity, and the brain. *Proc Natl Acad Sci U S A*. 1996;93(10):4529-4536. doi:10.1073/pnas.93.10.4529 [PMCID: PMC39311] [PubMed: 8643438] [CrossRef: 10.1073/pnas.93.10.4529]
18. Falcioni F, Ito K, Vidovic D, et al. . Peptidomimetic compounds that inhibit antigen presentation by autoimmune disease-associated class II major histocompatibility molecules. *Nat Biotechnol*. 1999;17(6):562-567. doi:10.1038/9865 [PubMed: 10385320] [CrossRef: 10.1038/9865]
19. Xia J, Siegel M, Bergseng E, Sollid LM, Khosla C. Inhibition of HLA-DQ2-mediated antigen presentation by analogues of a high affinity 33-residue peptide from alpha2-gliadin. *J Am Chem Soc*. 2006;128(6):1859-1867. doi:10.1021/ja056423o [PMCID: PMC2597451] [PubMed: 16464085] [CrossRef: 10.1021/ja056423o]
20. Hara M, Martinez-Hernandez E, Ariño H, et al. . Clinical and pathogenic significance of IgG, IgA, and IgM antibodies against the NMDA receptor. *Neurology*. 2018;90(16):e1386-e1394. doi:10.1212/WNL.0000000000005329 [PMCID: PMC5902781] [PubMed: 29549218] [CrossRef: 10.1212/WNL.0000000000005329]

21. Flanagan EP, Hinson SR, Lennon VA, et al. . Glial fibrillary acidic protein immunoglobulin G as biomarker of autoimmune astrocytopathy: analysis of 102 patients. *Ann Neurol*. 2017;81(2):298-309. doi:10.1002/ana.24881 [PubMed: 28120349] [CrossRef: 10.1002/ana.24881]
22. Basal E, Zalewski N, Kryzer TJ, et al. . Paraneoplastic neuronal intermediate filament autoimmunity. *Neurology*. 2018;91(18):e1677-e1689. doi:10.1212/WNL.0000000000006435 [PMCID: PMC6207411] [PubMed: 30282771] [CrossRef: 10.1212/WNL.0000000000006435]
23. Maudes E, Landa J, Muñoz-Lopetegui A, et al. . Clinical significance of Kelch-like protein 11 antibodies. *Neurol Neuroimmunol Neuroinflamm*. 2020;7(3):e666. doi:10.1212/NXI.000000000000666 [PMCID: PMC7051195] [PubMed: 31953318] [CrossRef: 10.1212/NXI.000000000000666]
24. Lucchinetti CF, Kimmel DW, Lennon VA. Paraneoplastic and oncologic profiles of patients seropositive for type 1 antineuronal nuclear autoantibodies. *Neurology*. 1998;50(3):652-657. doi:10.1212/WNL.50.3.652 [PubMed: 9521251] [CrossRef: 10.1212/WNL.50.3.652]
25. Kaneko A, Kaneko J, Tominaga N, et al. . Pitfalls in clinical diagnosis of anti-NMDA receptor encephalitis. *J Neurol*. 2018;265(3):586-596. doi:10.1007/s00415-018-8749-3 [PubMed: 29356973] [CrossRef: 10.1007/s00415-018-8749-3]

## Figures and Tables

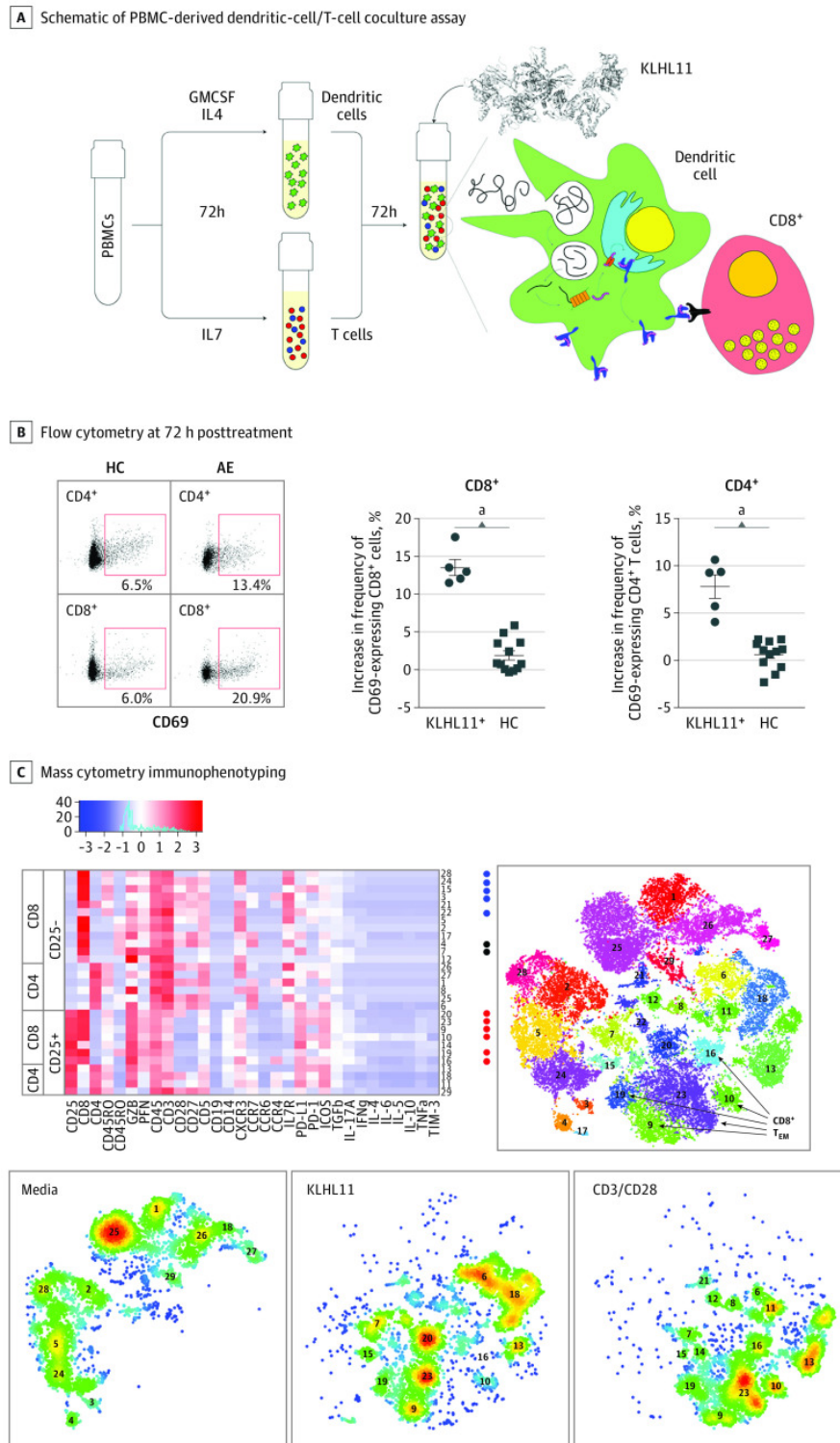
Figure 1.



### Examples of Magnetic Resonance Image (MRI) Abnormalities Found in the Central Nervous System, Cranial Nerves, and Spinal Nerve Roots of Patients With Autoimmune Kelch-like Protein-11 (KLHL11) Encephalitis

T2 hyperintensity involving the left medullary olive (arrowhead; A). Fluid-attenuated inversion recovery (FLAIR) hyperintensity involving the pons (B). FLAIR hyperintensity involving the midbrain (arrowhead, C). Leptomeningeal enhancement (arrowhead) around the vermis on T1 post-gadolinium images (D). T2 hyperintensity involving the right medial temporal lobe and atrophy of the left medial temporal lobe (E). Bilateral medial temporal hyperintensities (right greater than left; F). Gadolinium enhancement of the left trigeminal nerve (arrowhead) on axial and coronal sections (G). Gadolinium enhancement of the lumbosacral roots (arrowhead; H).

Figure 2.



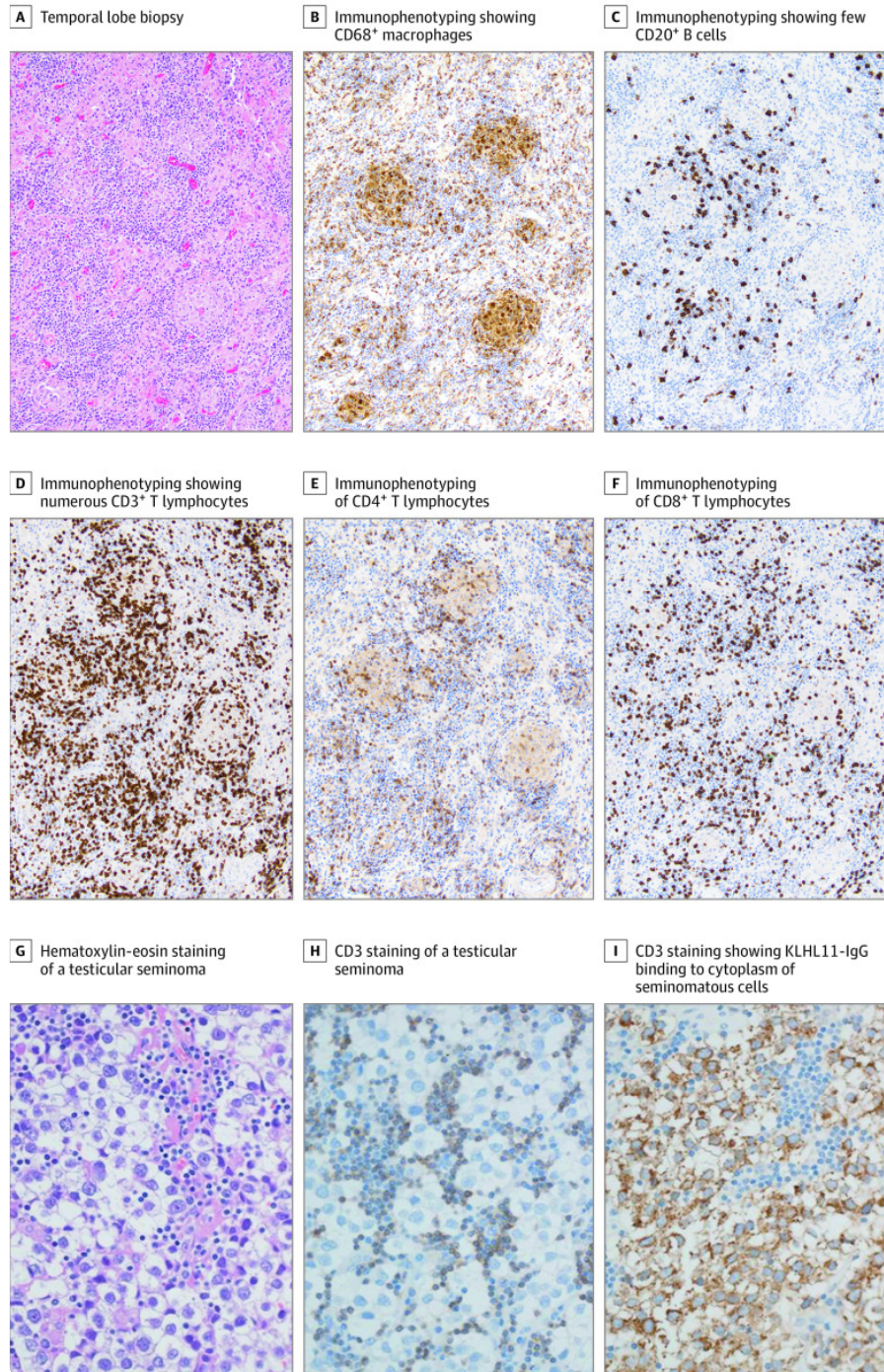
### Kelch-like Protein-11 (KLHL11)-Specific T-cell Response

Schematic of peripheral blood mononuclear cell-derived DC-T cell coculture assay (A). Flow cytometry at 72 hours following treatment demonstrated that (compared with vehicle treated cells) KLHL11 antigen-treated cells exhibited an increased frequency of CD69 expressing CD8<sup>+</sup> and CD4<sup>+</sup> T cells in KLHL11 immunoglobulin G seropositive (KLHL11<sup>+</sup>) patients but not healthy control (HC) individuals (B). Representative flow plots shown on left. Cytometry by time of flight immunophenotyping demonstrated an increased frequency of CD25 expressing CD4<sup>+</sup> and CD8<sup>+</sup> T cells following antigen treatment (C). Heat map shows expression of the indicated markers for each cluster. Rphenograph scatterplots show clusters generated by T-distributed stochastic neighbor embedding plots for all conditions (right) and for each condition (bottom panels).



<sup>a</sup>*P* < .001.

Figure 3.

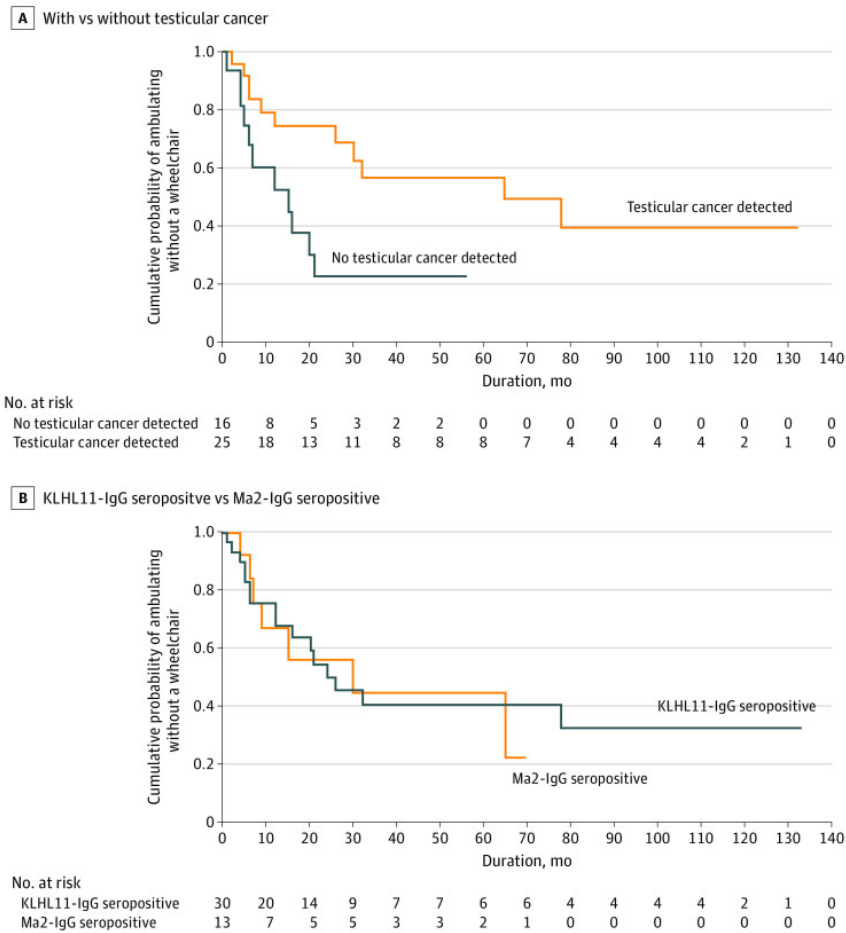


#### Immunohistochemical Staining of Brain Biopsy (A-F) and Testicular Seminoma (G-I)

Temporal lobe biopsy demonstrates nonnecrotizing granulomas, prominent lymphocytic infiltrates, and neuronal loss (A). Immunophenotyping demonstrated CD68-positive macrophages (B), fewer CD20-positive B cells (C) compared with numerous CD3+ T lymphocytes (D). Lymphocytes are both CD4+ (E) and CD8+ T cells (F). Hematoxylin-eosin (G) and CD3 (H) staining of a testicular seminoma from a patient with autoimmune Kelch-like protein 11 encephalitis demonstrates collection of inflammatory cells in the seminoma. Kelch-like protein 11 IgG binds to the cytoplasm of the seminomatous cells (I). Magnification 10× for panels A through F and 20× for G through I.



Figure 4.



**Clinical Outcomes Assesed Based on Wheelchair Dependence**

Kaplan-Meier curves show cumulative probability of ability to ambulate without wheelchair at last follow-up. A, Log-rank test:  $P = .01$ . B, Log-rank test:  $P = .93$ . KLHL11 indicates Klech-like protein 11.

## Table.

Comparison of Clinical and Radiological Findings in Patients With Autoimmune KLHL11 or Ma2 Encephalitis

Characteristic	No. (%)		P value
	KLHL11-IgG+ (N = 39) <sup>a</sup>	Ma2-IgG+ (N = 22)	
Male	39 (100)	16 (80)	.01
Age, median (range), y	46 (28-73)	43 (23-75)	.27
Cancer diagnosed <sup>b</sup>	25/36 (69)	9/18 (50)	.23
Seminoma	21/36 (58)	2/18 (11)	.001
Nonseminomatous germ cell tumor	2/36 (6)	6/18 (33)	.01
Rhombencephalitis	32 (82)	8 (40)	.003
Ataxia	32 (82)	6 (30)	<.001
Vertigo	21 (54)	3 (15)	.005
Sensorineural hearing loss	15 (39)	0	.001
Tinnitus	14 (36)	0	.001
Limbic encephalitis	7 (19)	8 (40)	.11
Seizures	9 (23)	10 (50)	.04
Altered mental status	16 (41)	15 (75)	.03
Narcolepsy	0	3 (15)	.04
Neuropathy	7 (18)	0	.08
Outcome measures			
Gait aid at last follow-up	21/34 (62)	7/13 (54)	.92
Clinical improvement/stabilization	20 (56)	8 (57)	.92
mRS at last follow-up, median (range)	4 (2-6)	4 (2-6)	.68
Change in mRS, median (range)	0 (-3 to 2)	0 (-4 to 2)	.86
Follow-up period, median (range), mo	30 (2-216)	19 (4-70)	.19

Abbreviations: KLHL11, Klech-like protein 11; mRS, modified Rankin Score.

<sup>a</sup>Thirteen patients previously reported.

<sup>b</sup>Patients who had diagnostic evaluation for occult malignancy, at least computed tomography of chest abdomen/pelvis, and testicular ultrasonography.